GAP-97-004, Auger project technical note.* Performance simulations of a 10 m^2 water Čerenkov detector and comparison with experiment.

Clement Pryke
Enrico Fermi Institute, University of Chicago, USA

January 9, 1997

Abstract

A detailed simulation of the radiation and collection of Čerenkov light in water tank detectors has been implemented. These detectors are proposed for the ground array of the Auger project — a next generation observatory of the highest energy cosmic rays. The simulation is described, and the results compared with muon calibration data from a prototype unit now operating at the AGASA array.

1 Introduction

It is proposed that the ground array systems of the northern and southern hemisphere Auger cosmic rays observatories will consist of ≈ 1600 water tank detectors arranged in a hexagonal grid with spacing of 1.5 km (covering an area of ≈ 3000 km^2) [1]. Each detector will be a 10 m^2 $\times$ 1.2 m deep cylindrical volume of water, lined with a diffusely reflective white material, and viewed vertically from above by 3 photomultiplier tubes (pmts) ≈ 200 mm in diameter.

*This paper was prepared for the proceedings of the ICRR International Symposium on Extremely High Energy Cosmic Rays held in Tokyo, Japan in September 1996.

Selection of these parameters has been carried out through Monte Carlo simulations. In an accompanying paper simulations of the complete ground array systems are described [2]. Here the water tank simulation element of the procedure is described and tested against single muon experimental data from a full scale prototype tank now operating at the AGASA array in Japan [3].

2 Physical properties

To make realistic calculations of water tank performance it is necessary to have knowledge of several things:

- The interaction behaviour of relativistic particles in water.
- The absorption length of light in water.
- The reflectivity of the lining material.
- The quantum efficiency, and photoelectron collection efficiency of the pmts being used.

The interactions of cosmic ray particles in water is well known physics; for details of the properties assumed in this work see [4]. The yield of Čerenkov light for track length dx and wavelength interval $d\lambda$ is

$$\frac{dN}{dxd\lambda} = \frac{2\pi\alpha}{\lambda^2}\left(1 - \frac{1}{\beta^2 n^2}\right) dxd\lambda,$$

where α is the fine structure constant, β is the particle velocity and n is the refractive index of water (1.33).

Figure 1 shows this function for a $\beta \approx 1$ particle together with the absorption length of pure, fresh water [5], the reflectivity of a diffusively reflecting material (Tyvec) [6], and the quantum efficiency of a bialkali photocathode [7]. The spectral distribution of the Čerenkov photons is analytic. The lining material reflectivity and pmt quantum efficiency are accurate measurements (caveat: Tyvec was measured in air, not water). By far the most uncertain quantity is the absorption length of the water. The curve shown was inferred from measurements of the clearest natural ocean waters; in fact

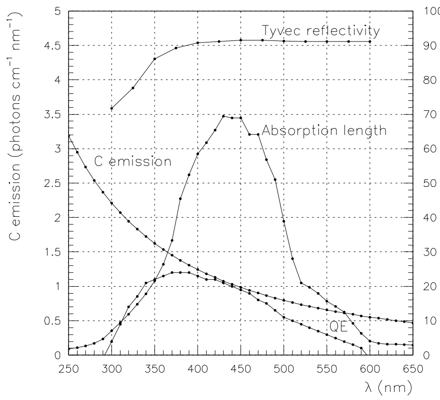

Figure 1: Important spectral characteristics for a water Čerenkov detector.

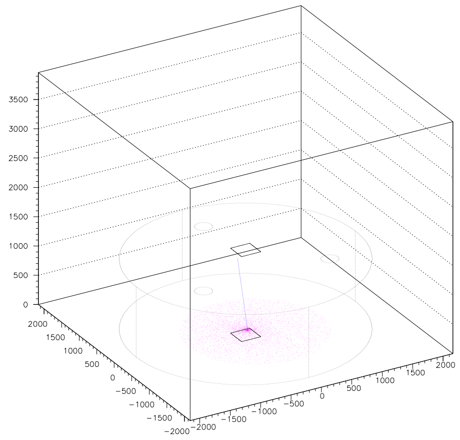

Figure 2: Tank simulation code in operation; a single muon track with photon first hits.

lab water can reach higher peak values [8]. However, particulate and dissolved impurities present in tank water of practical (long term) quality can be expected to alter not only the peak value (normalization) of the curve, but also its shape. In the context of possible problems with tank freezing it is interesting to note that for salt concentrations typical of ocean water there is no significant ($> 10\%$) loss of absorption length relative to pure, fresh water [5].

3 Simulation procedure

The simulation procedure is described in detail elsewhere [4]; briefly, each particle is tracked as it moves through the detector volume. At each increment step (5 mm) an appropriate number of Čerenkov photons are generated at an angle to the particle trajectory ($42°$ for $\beta \approx 1$), and each photon is ray-traced as it passes through the water, and reflects from the tank lining. When photons strike the photomultiplier tubes their arrival times are recorded.

The simulation code has recently been up-graded to include spectral effects in full detail. Each emitted photon is assigned a wavelength from the distribution shown in figure 1; the lining material reflectivity and pmt quantum efficiencies shown are also used. Since data is not available for the absorption length of the actual tank water we use the pure water shape, and re-normalize the peak height to a user selectable value. Collection efficiency for photoelectrons (pes) onto the first dynode is $\approx 60\%$ for the R1408 pmt in use on the prototype tank (assumed here to be wavelength independent). The pmts are approximated as circular areas in the plane of the detector top surface with area equal to the effective area of 200 mm pmts (530 cm^2).

To construct pmt output waveforms from a list of pe times it is necessary to have knowledge of the pulse shape and amplitude distribution for single pes. These have recently been measured for the ex-IMB R1408 units [9]. The simulation code sums single electron pulses to form an aggregate predicted pulse shape. Finally the time and voltage quantization of the 100 mega sample per second digital oscilloscope used to record data on the AGASA tank is simulated.

4 Comparison with experimental data

The prototype detector is equipped with a scintillator telescope consisting of two 0.1 m^2 paddles located vertically above and below the center of the detector. A list of incident muons is generated with a realistic distribution of energies and trajectories [10]. Figure 2 illustrates the operation of the simulation for a single incident particle.

The average time amplitude profile of muon telescope events is governed only by the water absorption length, lining material reflectivity and pmt single pe pulse shape; it is *not* affected by the absolute number of pes collected, only by their time dispersion. Since we believe the reflectivity and pulse shape to be well measured there remains only a single free parameter — the water absorption length. Adjusting the peak absorption length to 35 meters produces the fit between experimental data and simulation shown in figure 3[1]. This seems a high value since the tank was filled from the normal mains supply at Akeno, and recirculating filtration was not operating at the time this data was taken (July 26 1996). However after careful consideration it seems the only way to explain the 55 ns exponential decay constant of the

[1]The average muon pulse shape shown in figure 3 was obtained using the charge cut $Q < 250$ pC to exclude multi-particle events, and hence avoid possible distortions of the shape.

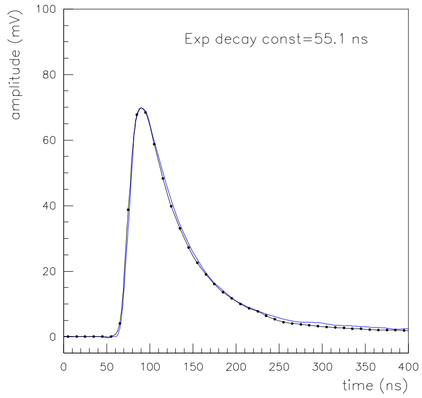

Figure 3: Average muon pulse shape. Data curve has points, other curve is simulation.

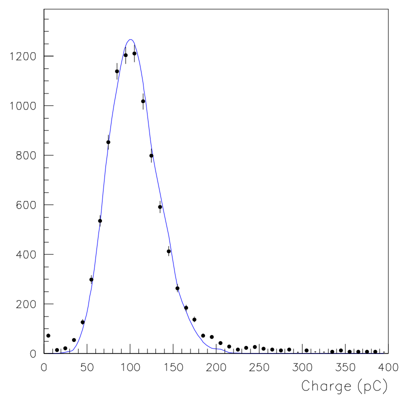

Figure 4: Muon charge distribution. Points are data, curve is simulation.

pulse back edge.

The shape of the charge distribution recorded for a batch of muon events is sensitive not only to the absolute number of pes, but also to the single electron charge spectrum of the pmt, and the details of the particle interaction physics. In figure 4 we can see that there is agreement for the central region of the distribution; it is probable that the high side tail present in the data for $150 < Q < 250$ pC is mainly due to δ-ray production [11] (an effect not included in the simulation at present). The extreme high tail events ($Q > 250$ pC) are presumably small air shower events. The simulation gives 30 collected photoelectrons per pmt with the material parameters as noted. This implies a gain of 2.1×10^7 to be compared to the data sheet value of $\approx 3 \times 10^7$ at the applied voltage (1.36 KV).

Finally, it is interesting to compare raw individual muon pulse shapes; figure 5 shows some real and simulated events. Note that the simulation reproduces the rich time structure apparent in the data. Figures 3, 4 and 5 show data from pmt number one; the other tubes give near identical results.

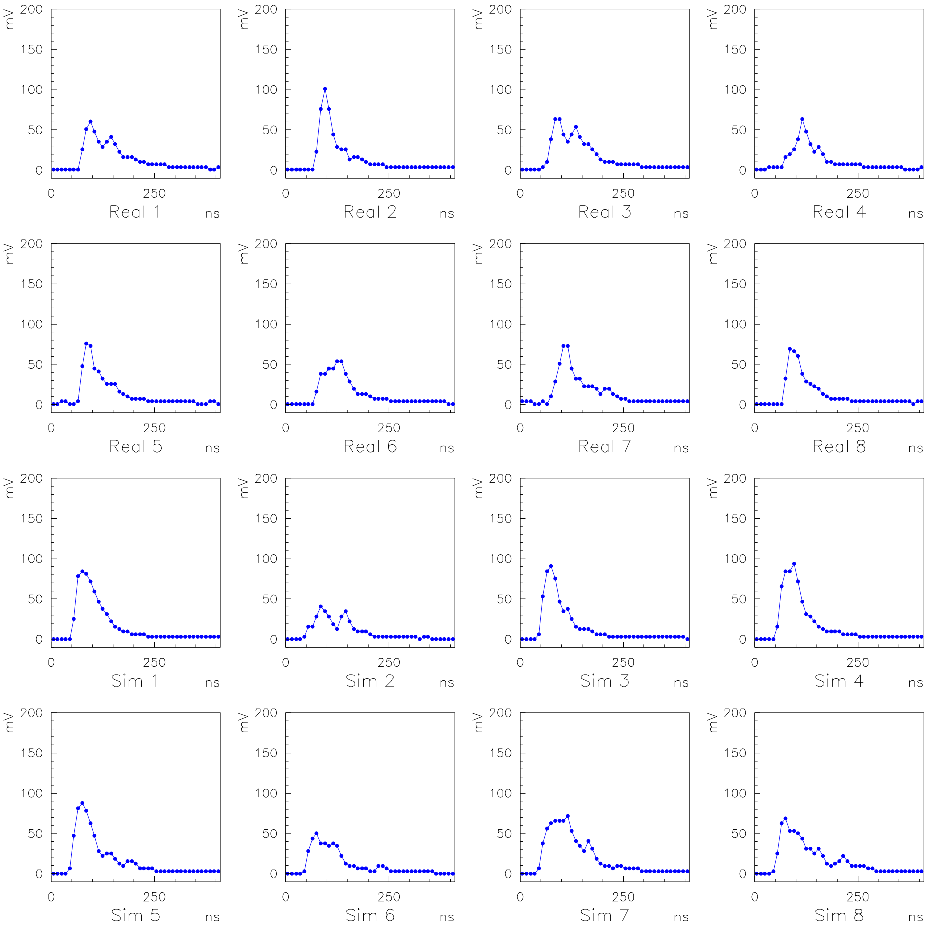

Figure 5: Raw single muon waveform traces from the AGASA water Čerenkov detector. The first eight real and simulated events are shown.

5 Conclusions

The detector and front end electronics elements of the Auger ground array simulation package have been tested against experimental data from a prototype tank, and the assumed water absorption length adjusted to provide a best fit to the decay time of the average muon pulse shape. With the material parameters stated, agreement is good for this, and several other comparisons. We thus have confidence that the simulation can be used to translate air shower simulations into ground array events, and hence to predict the performance of the proposed Auger experiment. At this time, more detailed and accurate measurements of tank water absorption length are needed.

6 Acknowledgements

Thanks is due to M. Nagano, N. Sakaki and the entire AGASA group for constructing the prototype water tank, and providing the experimental data used in this paper.

References

[1] The Auger Collaboration, "Design Report", FNAL, (1995).

[2] C. Pryke, These proceedings.

[3] N. Sakaki, These Proceedings.

[4] C. Pryke, PhD thesis, University of Leeds, (1996). Available from ftp://hep.uchicago.edu/pub/auger/pryke/clp_thesis.ps.gz

[5] R. Smith and K. Baker, App. Optics, **20** (1981) 177.

[6] Surface Optics Corporation, Report SOC-R950-001-0195.

[7] Hamamatsu Photonics, R1408 Technical Data Sheet, (1985).

[8] S. Noel and H. Mes, SNO tech. note SNO-STR-91-062,

[9] C. Pryke and T. Kutter, Auger tech. note GAP-96-041, Available from ftp above.

[10] T. Gaisser, “Cosmic Rays and Particle Physics”, Cambridge University Press, page 71 (1990).

[11] G. Yodh et al, MILAGRO technical note, (Nov 1996).